Doubly Encapsulated Perylene Diimides: Effect of Molecular Encapsulation on Photophysical Properties

Jeroen Royakkers,[†] Alessandro Minotto,[‡] Daniel G. Congrave,[†] Weixuan Zeng,[†] Adil Patel,[‡] Andrew D. Bond,[†] Dejan-Krešimir Bučar,[§] Franco Cacialli,[‡] and Hugo Bronstein*,[†,⊥]

[†]Department of Chemistry, University of Cambridge, Lensfield Road, Cambridge CB2 1EW, United Kingdom
[⊥]Cavendish Laboratory, University of Cambridge, Cambridge CB3 0HE, United Kingdom
[‡]Department of Physics and Astronomy and LCN, University College London, Gower Street, London WC1E 6BT, United Kingdom
[§]Department of Chemistry, University College London, 20 Gordon Street, London WC1H 0AJ, United Kingdom

S *Supporting Information*

ABSTRACT: Intermolecular interactions play a fundamental role on the performance of conjugated materials in organic electronic devices, as they heavily influence their optoelectronic properties. Synthetic control over the solid state properties of organic optoelectronic materials is crucial to access real life applications. Perylene diimides (PDIs) are one of the most highly studied classes of organic fluorescent dyes. In the solid state, $\pi-\pi$ stacking suppresses their emission, limiting their use in a variety of applications. Here, we report the synthesis of a novel PDI dye that is encapsulated by four alkylene straps. X-ray crystallography indicates that intermolecular $\pi-\pi$ stacking is completely suppressed in the crystalline state. This is further validated by the photophysical properties of the dye in both solution and solid state and supported by theoretical calculations. However, we find that the introduction of the encapsulating "arms" results in the creation of charge-transfer states which modify the excited state properties. This article demonstrates that molecular encapsulation can be used as a powerful tool to tune intermolecular interactions and thereby gain an extra level of control over the solid state properties of organic optoelectronic materials.
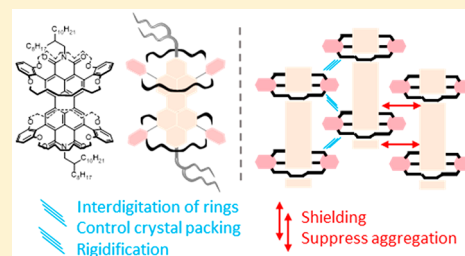
INTRODUCTION

Perylene diimides (PDIs) are one of the most highly studied classes of organic fluorescent dyes.[1] They were initially primarily used as high-grade colorants in the pigment and textile industry but have recently attracted great interest as materials for application in optoelectronic devices such as organic solar cells (OSCs), light-emitting diodes (OLEDs), transistors, and lasers.[1−3] The widespread use of PDI derivatives can be mainly attributed to their desirable optoelectronic properties (e.g., high photoluminescence quantum yields (PLQYs), tunable absorption and emission and high electron mobilities), photothermal stability, and synthetic versatility.[3]

However, PDI chromophores have an inherently strong propensity to aggregate through $\pi-\pi$ stacking.[4] While sometimes desirable for certain properties such as charge transport, this also limits their potential applications because it can greatly diminish their photoluminesence at higher concentrations or in the solid state.[4−6] As a result, it is extremely important to enhance our understanding of the structure−property relationships in PDIs toward obtaining higher levels of control over their aggregation behavior and photophysical properties in both the solution and solid state.

Overall, there are three major strategies to suppress aggregation through $\pi-\pi$ stacking in PDI dyes. The first approach relies on the incorporation of steric bulk at the bay positions (1, 6, 7, 12) of the perylene core. Sterically demanding moieties can be incorporated via the facile nucleophilic aromatic substitution (S_NAr) of halogenated PDI cores.[7,8] Although incorporating steric hindrance at the bay positions reduces $\pi-\pi$ stacking, it commonly imparts a twist in the planar aromatic PDI core.[9,10] This can undesirably influence the photophysical properties of the dye.[11]

Alternatively, it is also possible to shield the PDI core from intermolecular communication without disrupting its planarity through functionalizing the imide positions with bulky substituents that shield both faces of the aromatic perylene.[12] This method was recently demonstrated by Wong and coworkers.[4] They reported the synthesis of a series of PDI derivatives with varying degrees of bulk on the imide positions, ranging from simple phenyl moieties to more congested 3,5-di-*tert*-butylphenyl and trityl groups.[4] While their crystallographic data confirm that increasing the bulk of the substituents leads to more spatially shielded dyes, the UV−vis absorption data still indicate significant aggregation for these molecules.[4] Therefore, incorporating bulky groups at the imide positions of PDIs does not completely preclude the formation of

Scheme 1. Synthesis of the Doubly-Encapsulated Perylene Diimide (PDI-Encap)
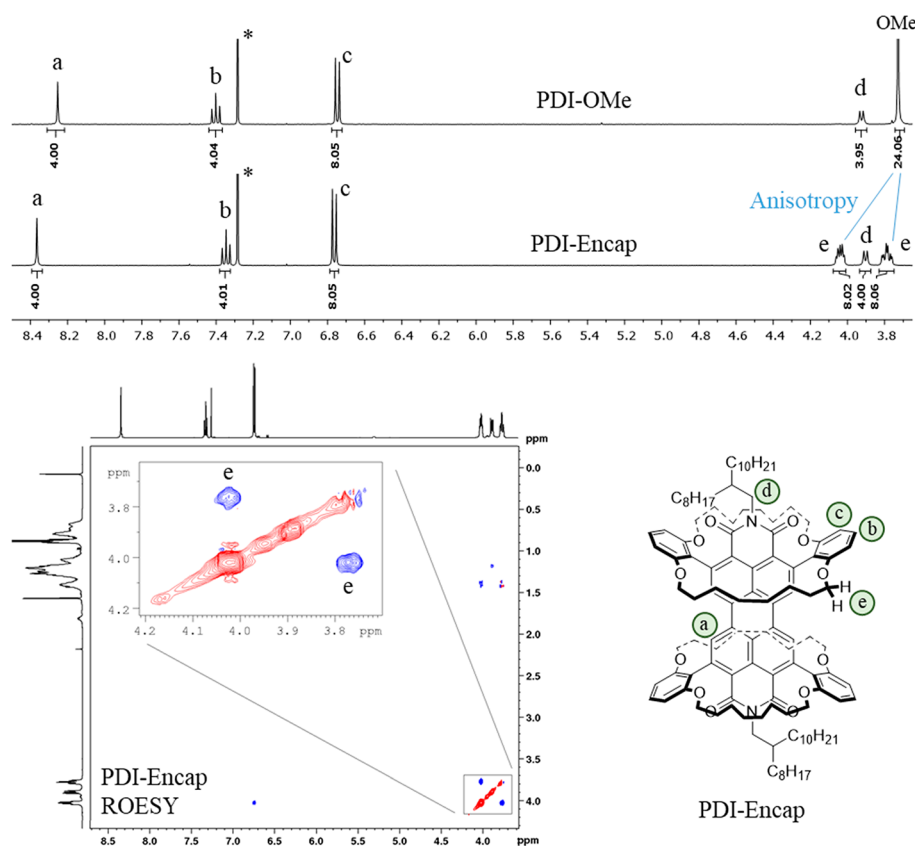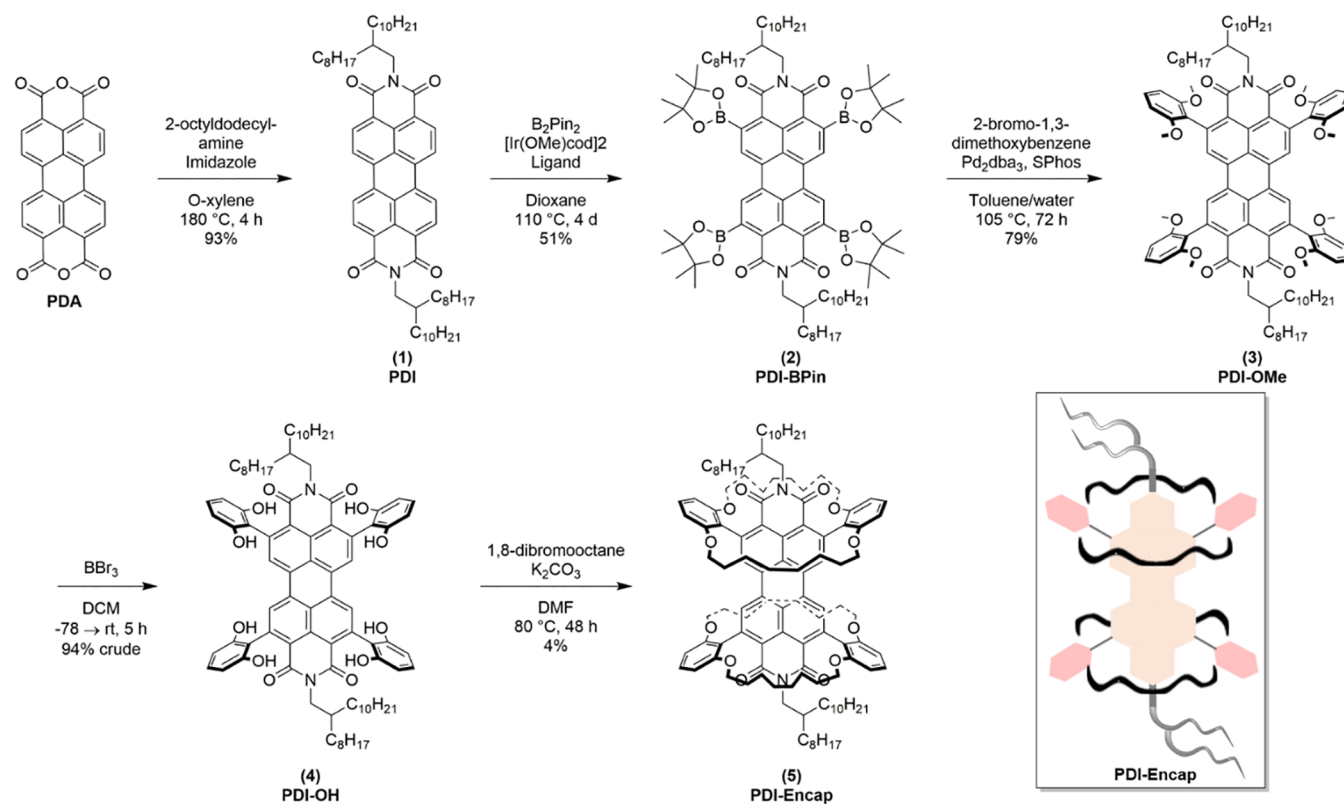
Figure 1. (top) Fragment of ^{1}H NMR spectra of **PDI-OMe** and **PDI-Encap**. (bottom left) ^{1}H−^{1}H ROESY spectrum of **PDI-Encap**. (bottom right) Structural NMR assignment. The shifts are reported in ppm and referenced against residual CHCl$_3$ in CDCl$_3$.

aggregates and hence offers only limited control over their photophysical properties.

As a third option, we propose a strategy whereby the PDI core is surrounded by encapsulating alkylene straps, as has been demonstrated in other conjugated materials.[13−22] This method makes use of recently developed chemistry on the ortho-positions (2, 5, 8, 11) of PDIs[23,24] to install 1,3-dimethoxybenzene groups. These are then further functionalized to fully sheath the PDI core with two encapsulating rings. This article discusses the synthesis of a novel, doubly encapsulated PDI and investigates the structural influence of molecular encapsulation on the photophysical properties of the PDI chromophore.

■ SYNTHESIS AND CHARACTERIZATION

The synthesis of the doubly encapsulated perylene diimide (**PDI-Encap**) is demonstrated in Scheme 1. Perylene-3,4,9,10-tetracarboxylic dianhydride (**PDA**) was reacted with 2-octyldodecylamine to form the corresponding **PDI** (**1**) in 93% yield after column chromatography. Upon iridium-catalyzed direct tetraborylation, **PDI-BPin** (**2**) was formed in a respectable yield of 51%. During the direct borylation reaction, the catalyst is expected first to coordinate to one of the carbonyl oxygens, which is then used to direct the BPin groups onto the ortho positions of the perylene core through a concerted metalation deprotonation.[23] The cycle repeats itself until all four BPin groups are installed.[23] Further reaction with 2-bromo-1,3-dimethoxybenzene under standard Suzuki−Miyaura cross coupling conditions with Pd_2dba_3 and SPhos afforded the tetra-arylated product **PDI-OMe** (**3**) in excellent yield (79%). SPhos was selected as the preferred ligand together with Pd_2dba_3 considering their outstanding efficiency at coupling sterically encumbered substrates.[25] **PDI-OMe** was then subjected to a demethylation with BBr_3 to afford the **PDI-OH** as a crude product. The subsequent encapsulation with 1,8-dibromooctane, using high-dilution and basic conditions, gave the final, doubly encapsulated perylene diimide (**PDI-Encap**) as the only isolable product in 4% yield after column chromatography. This yield, although low, is quite reasonable considering that eight S_N2 reactions are taking place within one step and that intermolecular or polymeric products can be formed during the process.

NMR Spectroscopy. Both **PDI-OMe** and **PDI-Encap** were fully characterized via NMR, X-ray crystallography, HRMS, and/or elemental analysis. The aromatic regions (6.6−8.4 ppm) in the ^1H NMR spectra of **PDI-OMe** and **PDI-Encap** are very similar (Figure 1, top), displaying three signals (labeled a, b, and c) corresponding to the protons of the PDI core and peripheral phenyl groups, respectively. However, a significant difference is observed in the alkoxy region (3.6−4.1 ppm). **PDI-OMe** displays a singlet (labeled OMe) which integrates to 24 protons, as expected. For **PDI-Encap** the same signal is split into two multiplets (labeled e) which each integrate to 8 protons. Further information was gathered through 2D NMR experiments. $^1H−^{13}C$ HSQC data indicate that both proton environments (e) correlate to the same carbon atom (Figure S12), suggesting that they undergo slow conformational/chemical exchange. This is confirmed by $^1H−^1H$ ROESY NMR (Figure 1, bottom left) and is indicative of conformational restriction of the alkoxy chains as a result of encapsulation. Furthermore, the proton signals corresponding to the alkylene straps are highly shielded (<0.9 ppm), indicating that these environments are proximal to the π system of the PDI chromophore, as expected upon encapsulation (Figure S8).

X-ray Crystallography. Single crystal X-ray diffraction analysis of **PDI-Encap** unambiguously proved that the alkylene moieties of the peripheral aryl groups engage in horizontal encapsulation rather than in vertical looping or cross encapsulation (Figures 2 and 3). Surprisingly, neither of these possible side-products could be isolated (Figure 2), although their formation cannot be precluded due to the low yield of **PDI-Encap**. **PDI-Encap** crystallizes in the triclinic $P\bar{1}$ space group with one-half of a **PDI-Encap** molecule and one $CHCl_3$
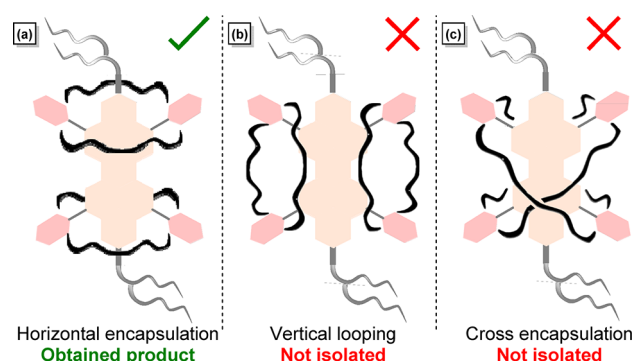
Figure 2. Graphical representation of the potential encapsulation products (excluding intermolecular products). (a) Observed horizontal encapsulation. (b) Nonisolated vertical looping. (c) Nonisolated cross encapsulation.
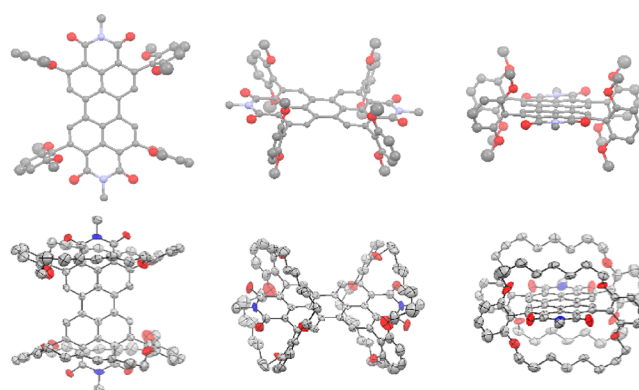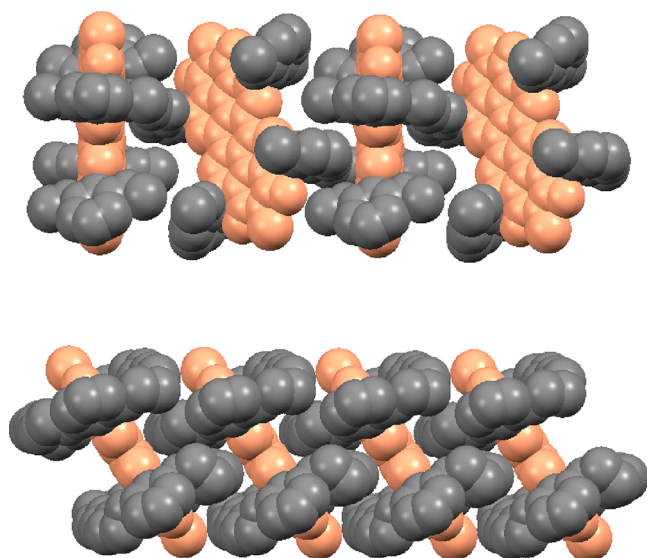

Figure 3. Molecular structures of **PDI-OMe** (top) and **PDI-Encap** (bottom) derived from single crystal X-ray diffraction data of the respective meso compounds viewed from three different perspectives. The branched octyldodecyl chains, all hydrogen atoms, and solvent molecules are omitted for clarity.

molecule in the asymmetric unit. The **PDI-Encap** molecules stack along the crystallographic a axis in an offset manner, exhibiting 9.9 Å centroid-to-centroid separation distances between adjacent PDI cores (Figure 4). The axes and planes of the PDI cores, belonging to neighboring **PDI-Encap** molecules, are aligned in parallel. Notably, the packing of the **PDI-Encap** molecules is not driven by π−π interactions, which is in contrast to conventional PDI dyes that regularly engage in π-stacking in the crystalline state.[26,27] Instead, it appears that the chromophore orientation is dictated by the crystallization of the encapsulating chains (Figure 4). The absence of π−π interactions in the **PDI-Encap** crystal structure is clearly attributable to steric hindrances caused by the peripheral aryl groups and the horizontally aligned alkylene chains.

The structurally related tetra-arylated perylene (**PDI-OMe**) crystallizes in the monoclinic $P2_1/c$ space group with one **PDI-OMe** and two $CHCl_3$ molecules in the asymmetric unit. The **PDI-OMe** molecules stack along the (011) Miller plane (Figure 4), whereby its PDI cores display 10.2 Å centroid-to-centroid separation distances. The planes of neighboring PDI cores close at an angle of 58° (Figure 4). The molecular stacks are stabilized by C−H···π and C−H···O interactions in the absence of π−π interactions, which is, similar to **PDI-Encap**, caused by steric hindrances of the peripheral aryl groups.

The stark differences between the stacking of the PDI cores in the crystal structures of **PDI-Encap** and **PDI-OMe** suggest that the spacing and the alignment of the encapsulating alkylene groups in **PDI-Encap** promote molecular interdigitation and the parallel alignments of its PDI cores. Alkylene encapsulation might, therefore, provide an approach not only for suppressing π−π stacking as they are

Figure 4. X-ray crystal structures of molecular stacks of: **PDI-OMe**, viewed along the (100) Miller plane (top), and **PDI-Encap**, viewed along the (01$\bar{1}$) Miller plane (bottom). The branched octyldodecyl chains, all hydrogen atoms, and solvent molecules are omitted for clarity. Color scheme: PDI cores, orange; peripheral aryl and encapsulating alkylene groups, gray.

most commonly used,[13,14,16−21] but also to control the arrangement of fluorophores in the solid state.

RESULTS AND DISCUSSION

Photophysical Results. The solution and thin film absorption spectra of **PDI**, **PDI-OMe**, and **PDI-Encap** are presented in Figure 5. The spectral profiles of the solution
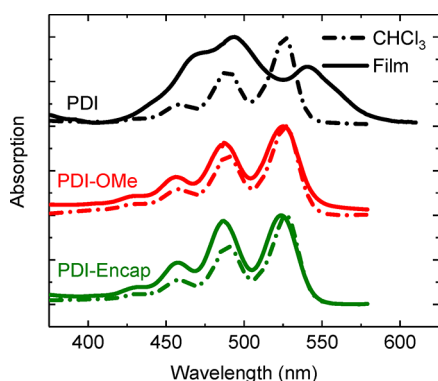

Figure 5. UV−vis absorption spectra of **PDI** (black), **PDI-OMe** (red), and **PDI-Encap** (green) in both solution and thin film.

absorption spectra are near-identical for the three dyes. They consist of four well-resolved vibronic bands at ~430, ~460, ~485, and ~530 nm (λ_{max}) corresponding to the 0−3′, 0−2′, 0−1′, and 0−0′ transitions, respectively. For the literature "PDI" dye, some vibronic fine structure is lost in the thin film spectrum, and the spectrum is red-shifted compared to the solution data. The observed broadening for **PDI** is ascribed to aggregation in the solid-state; a phenomenon that is typical for most perylene diimides.[26,27] These observations are in stark contrast to what is observed for **PDI-OMe** and **PDI-Encap**. In spin coated thin films, **PDI-OMe** and **PDI-Encap** retain more or less the same absorption profile as in solution, indicating

unimolecular behavior and showing that the formation of aggregates is suppressed. The sharper onset of absorption for the thin film of **PDI-Encap** compared to **PDI-OMe** suggests that it is more rigid and less prone to conformational disorder in the solid state.[13,28,29]

The absorption and photoluminescence (PL) spectra of the three dyes in solution (Figures 5 and 6) display the typical
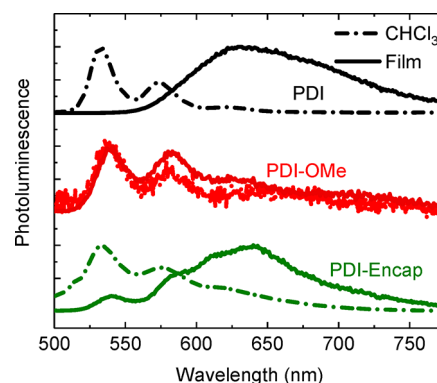
Figure 6. Photoluminescence spectra of **PDI** (black), **PDI-OMe** (red), and **PDI-Encap** (green) in both solution and thin film.

mirror image behavior that is established for rigid luminophores that emit from π−π* states.[30] However, we note that the PL spectra for **PDI-OMe** and **PDI-Encap** are broader than that of **PDI** with more poorly resolved vibronic fine structures and shallower onsets (Figure 6). This is suggestive of a degree of intramolecular charge transfer (ICT) character in their excited states, specifically between their electron-rich peripheral aryl rings and electron-deficient PDI cores. This is supported by the density functional theory (DFT) calculations discussed below, as well as by time-resolved PL data (Figures S17−22 and Table S1).

In solution, **PDI** displays a simple monoexponential decay with a lifetime (τ) of ~4 ns which can be ascribed to fluorescence from a π−π* state. In contrast, **PDI-OMe** and **PDI-Encap** display biexponential decays, consisting of a fast-decaying component (i.e., on a subnanosecond time scale) followed by the decay of a longer-lived state (τ = 3.4 and 2.3 ns for **PDI-OMe** and **PDI-Encap**, respectively). These data indicate that multiple states/processes contribute to the PL decay of **PDI-OMe** and **PDI-Encap**. The presence of a fast (nonradiative) decay component for **PDI-OMe** and **PDI-Encap** is responsible for their low solution PLQYs (<1%) compared to that of **PDI** (67%). As these spectra were taken from solutions, we propose that PL quenching (for the partially and doubly encapsulated dyes) originates from fast formation of ICT states with reduced luminescence efficiency, as supported by DFT calculations (*vide infra*).

The profiles of the thin film PL spectra for the dyes differ strongly among one another (Figure 6). In the case of **PDI**, the PL is much broader (~550−800 nm) and significantly less structured in the solid state than in solution but retains a PLQY of ~20%. This can be ascribed to emission from intermolecular species, whose formation is confirmed by the UV−vis data (Figure 5). However, the biexponential nature (τ_1 = 1.6 ns, τ_2 = 5 ns) of the PL decay (Table S1) suggests that the nature of such emissive aggregates is heterogeneous and might be partially excimeric. Indeed, formation of excimers is supported by the literature on similarly stacked perylene

bisimides.[31−34] In such systems, excimers can favor fast (subnanosecond) charge separation/radical formation,[35] which is ultimately responsible for the unusually fast (∼5 ns) excimeric emission observed from PDI films.

PDI-OMe and **PDI-Encap** display low thin film PLQYs (<1%) in-line with their low intrinsic solution PLQYs. Therefore, their thin film PL is vestigial, which complicates unambiguous assignment of their spectral features. Nevertheless, we note that the PL spectrum of **PDI-OMe** displays vibrational fine-structure and suppressed aggregate/excimer emission. Such a suppression is likely due to the orthogonal crystal packing of **PDI-OMe** observed during crystallographic structural analyses (Figure 4), which prevents intermolecular interactions both in the ground state (in agreement with thin film UV−vis data) as well as in the excited state. In contrast, the PL spectrum of **PDI-Encap** displays some fine structure but also a significantly broadened band at longer wavelengths. As thin film UV−vis data suggest that aggregation is largely suppressed for **PDI-Encap**, this is ascribed to an admixture of $\pi-\pi^*$ and ICT emission, which is also in agreement with the DFT data below.

Theoretical DFT Calculations. DFT/time-dependent DFT (TD-DFT) calculations at the level of B3LYP/6-31G*[36] were carried out to gain further insight into the surprising photophysical properties of **PDI-OMe** and **PDI-Encap**. For the gas phase optimized geometries of both dyes, the highest occupied molecular orbital (HOMO) and lowest unoccupied molecular orbital (LUMO) are each delocalized across the core of the PDI chromophore, while the first eight lower lying occupied molecular orbitals (HOMO−1 to HOMO−8) are all localized on the electron-rich peripheral dialkoxybenzene groups (HOMO−LUMO DFT results, Supporting Information). TD-DFT shows that the transitions to the 5 lowest singlet states of **PDI-Encap** can all be predominantly assigned to charge transfer from the peripheral aryl rings to the PDI core (HOMO−1−5 → LUMO) with no significant local excitation (HOMO → LUMO) of the PDI chromophore (Table S6). This greatly contrasts with the data calculated for some highly emissive literature PDI derivatives.[23] For both a simple *N*-alkylated PDI and a PDI tetra-arylated with electron-poor *p*-benzonitriles at the 2,5,8,11- positions, the $S_0 \rightarrow S_1$ transition is predominantly assigned to local excitation of the PDI chromophore (HOMO → LUMO) (Table S2 and S3). Therefore, we propose that fluorescence from the luminophoric PDI core of **PDI-Encap** and **PDI-OMe** is quenched by intramolecular charge transfer (ICT) between the electron-rich peripheral aryl groups and the PDI core, leading to the low observed PLQYs.

To gain a deeper understanding of the thin film PL results, we also performed TD-DFT calculations on the crystal structure geometries (Tables S5 and S7). We expect the gas phase structures to be representative of the average ground state geometry in solution, while the crystal structure geometries should be more representative of the thin film. For **PDI-Encap** in the gas phase optimized geometry, the lowest energy transition displaying a strong oscillator strength (ca. 0.42) is the local HOMO → LUMO $\pi-\pi^*$ transition ($S_0 \rightarrow S_5$, Table S6). The same is predicted for **PDI-OMe** ($S_0 \rightarrow S_3$, Table S4). These data correlate well with the solution PL spectra which display well-resolved vibronic fine structures (Figure 6). There is greater contrast between the TD-DFT data obtained for the crystal structure geometries of **PDI-Encap** and **PDI-OMe**. The data for **PDI-OMe** are very similar

for the gas phase and crystal structure geometries, i.e. the lowest energy transition with a strong oscillator strength (ca. 0.34, $S_0 \rightarrow S_4$, Table S5) is $\pi-\pi^*$ in nature. Therefore, the spectral features of the PL for **PDI-OMe** are very similar in solution and film (Figure 6). Conversely, while the lowest energy $\pi-\pi^*$ transition ($S_0 \rightarrow S_5$, Table S7) retains the gas phase oscillator strength (ca. 0.48) and approximate energy in the crystal structure geometry of **PDI-Encap**, an ICT transition ($S_0 \rightarrow S_3$, Table S7) at lower energy with a high oscillator strength (ca. 0.19) is also predicted. This transition is ascribed to the broad low energy PL band that is observed for the thin film of **PDI-Encap**.

To further differentiate between **PDI-OMe** and **PDI-Encap**, we also analyzed the low frequency vibration modes (<20 cm⁻¹) of both molecules (Supporting Information, Vibration Modes and Frequencies). It was found that **PDI-OMe** has six different low frequency vibration modes which are mainly attributed to the peripheral aryl rings, whereas **PDI-Encap** only has three modes which arise from vibrations caused by the alkylene straps. These data suggest that there is a higher rate of nonradiative decay for **PDI-OMe** than for **PDI-Encap**, in agreement with what can be reasonably inferred from the fluorescence lifetime data. Hence, the encapsulating straps are preferable.

■ CONCLUSIONS

In conclusion, we successfully prepared a novel, doubly encapsulated perylene diimide molecule, in which intermolecular aggregation is suppressed in both solution and the solid-state. This study therefore demonstrates that molecular encapsulation can be used as a three-dimensional tool to control intermolecular interactions. Furthermore, as opposed to shielding with bulky substituents, encapsulation can provide additional advantages because it can also rigidify molecular architectures as well as direct molecular assembly processes. However, because the encapsulation strategy used electron-rich peripheral aryls, we introduced charge transfer character into our molecule which thereby led to photoluminescence quenching. The work therefore highlights both the power of encapsulation as a synthetic tool for chromophore control but also their potential noninnocence with regards to underlying photophysical properties.

■ EXPERIMENTAL SECTION

All reactions were performed in predried glassware under argon atmosphere and with magnetic stirring unless stated otherwise and heated using an oil bath. Light-sensitive reactions were covered in foil. Chemicals were purchased from chemical suppliers (Sigma-Aldrich, TCI, Acros Organics, Alfa Aesar, SLS, Fisher Scientific and Fluorochem) and used as received unless stated otherwise. The reactions were monitored through thin layer chromatography (TLC) using DC Fertigfolien ALUGRAM aluminum sheets coated with silica gel. Column chromatography was carried out using Geduran silica gel 60 (40−63 μm) or Biotage Isolera Four with Biotage SNAP/SNAP ultra cartridges (10, 20, 50, or 100 g). ¹H NMR spectra were recorded on a 400 MHz Avance III HD Spectrometer, 400 MHz Smart Probe Spectrometer, or a 500 MHz DCH Cryoprobe Spectrometer in the stated solvent using residual protic solvent $CHCl_3$ (δ = 7.26 ppm, s) or DMSO (δ = 2.50 ppm, s) as the internal standard. ¹H NMR chemical shifts are reported to the nearest 0.01 ppm and quoted using the following abbreviations: s, singlet; d, doublet; t, triplet; q, quartet; qn, quintet; sxt, sextet; m, multiplet; br, broad; or a combination of these. The coupling constants (J) are measured in Hertz. ¹³C NMR spectra were recorded on the 500 MHz DCH Cryoprobe Spectrometer in the stated solvent using the residual protic solvent

CHCl3 (δ = 77.16 ppm, t) or DMSO (δ = 39.52 ppm, s) as the internal standard. ^{13}C NMR chemical shifts are reported to the nearest 0.1 ppm or 0.01 ppm if they cannot be distinguished. Mass spectra were obtained using a Waters LCT, Finnigan MAT 900XP or Waters MALDI micro MX spectrometer at the Department of Chemistry, University of Cambridge.

Synthesis of N,N′-Bis(2-octyldodecyl)-perylene-3,4,9,10-bis-(dicarboxidamide) (PDI).[37] Under argon, a mixture of 3,4,9,10-perylenetetracarboxylic dianhydride (3.00 g, 7.6468 mmol), 2-octyldodecylamine (5.60 g, 18.8190 mmol), o-xylene (13.5 mL), and imidazole (4.12 g, 60.5170 mmol) was stirred at 180 °C for 4 h. Upon cooling to room temperature, MeOH (∼100 mL) was added to the reaction mixture, and it was sonicated and filtered. The red-colored, clumpy solids were sonicated in MeOH and filtered three more times to obtain a more fine, red powdered solid. Lastly, the crude product was purified via column chromatography on silica using DCM and hexane (gradual column; 50% → 100% DCM). The product was obtained as a red solid (6.80 g, 7.1471 mmol, 93%). ^{1}H NMR (400 MHz, CDCl$_3$) δ 8.64 (d, J = 8.0 Hz, 4H), 8.56 (d, J = 8.1 Hz, 4H), 4.14 (d, J = 7.2 Hz, 4H), 2.01 (s, 2H), 1.29 (dd, J = 55.7, 14.7 Hz, 64H), 0.84 (t, J = 6.7 Hz, 12H). HRMS (ASAP-TOF): Calculated for C$_{64}$H$_{91}$N$_2$O$_4^+$: 951.6970. Found m/z 951.6979 [M + H]$^+$. The spectroscopic data is supported by the literature.[37]

Synthesis of N,N′-Bis(2-octyldodecyl)-2,5,8,11-tetrakis-(4,4,5,5-tetramethyl-1,3,2-dioxaborolan-2-yl)-perylene-3,4,9,10-tetracarboxylic Acid Diimide (PDI-BPin). In a glovebox, PDI (5.00 g, 5.2552 mmol), [Ir(OMe)cod]$_2$ (105.0 mg, 0.1584 mmol), tris(pentafluorophenyl)phosphine (336.3 mg, 0.6319 mmol), and bis(pinacolato)diboron (10.6786 g, 42.0517 mmol) were stirred in dry dioxane (125 mL) at 110 °C for 4 days. The solvent was removed under reduced pressure, and the residue was purified by trituration from hot ^{i}PrOH and a minimal amount of DCM. After cooling to room temperature, the solids were collected by filtration. The product was obtained as a red solid (3.8963 g, 2.6774 mmol, 51%). ^{1}H NMR (500 MHz, CDCl$_3$) δ 8.53 (s, 4H), 4.06 (d, J = 6.8 Hz, 4H), 1.97 (s, 2H), 1.55 (s, 48H), 1.45−1.21 (m, 64H), 0.87 (dd, J = 7.0, 6.3 Hz, 12H). ^{13}C NMR{H} (125 MHz, CDCl$_3$) δ 165.7, 138.7, 133.5, 128.1, 126.9, 126.6, 126.1, 84.7, 44.6, 36.8, 32.12, 32.08, 32.0, 30.2, 29.9, 29.5, 26.4, 25.2, 22.9, 14.3. HRMS (ASAP-TOF): Calculated for C$_{88}$H$_{135}$B$_4$N$_2$O$_{12}^+$: 1456.0394. Found m/z 1456.0387 [M + H]$^+$. Anal. Calcd. for C$_{88}$H$_{134}$B$_4$N$_2$O$_{12}$: C, 72.63; H, 9.28; N, 1.92. Found: C, 72.55; H, 9.30; N, 2.16 (average of two runs).

Synthesis of N,N′-Bis(2-octyldodecyl)-2,5,8,11-tetrakis(2-(1,3-dimethoxybenzene))perylene-3,4,9,10-tetracarboxylic Acid Diimide (PDI-OMe). Under argon, PDI-BPin (3.60 g, 2.4737 mmol), Pd$_2$dba$_3$ (453.0 mg, 0.4947 mmol), K$_2$CO$_3$ (3.4189 g, 24.7370 mmol), Sphos (434.3 mg, 1.0600 mmol), and 2-bromo-1,3-dimethoxybenzene (18.0310 g, 83.0688 mmol) were stirred in toluene (144 mL) and water (36 mL) at 105 °C for 72 h. After cooling to room temperature, water was added, and the reaction mixture was extracted with DCM (2×). The organic layers were washed with brine, dried over MgSO$_4$, and concentrated in vacuo. The crude product was purified by column chromatography on silica using DCM. Next, the solids were triturated from hot ^{i}PrOH and a minimal amount of DCM and collected by filtration. Lastly, the product was sonicated in methanol, collected by filtration, and dried in vacuo to afford orange colored solids (2.9106 g, 1.9455 mmol, 79%). ^{1}H NMR (500 MHz, CDCl$_3$) δ 8.23 (s, 4H), 7.38 (t, J = 8.4 Hz, 4H), 6.72 (d, J = 8.5 Hz, 8H), 3.90 (d, J = 7.5 Hz, 4H), 3.70 (s, 24H), 1.88−1.77 (m, 2H), 1.26−1.13 (m, 64H), 0.85 (td, J = 7.0, 5.2 Hz, 12H). ^{13}C NMR{H} (125 MHz, CDCl$_3$) δ 163.1, 156.8, 140.4, 133.6, 131.4, 129.1, 128.4, 125.9, 122.0, 120.7, 104.5, 56.1, 44.0, 36.2, 32.06, 32.05, 31.2, 30.4, 29.9, 29.82, 29.80, 29.51, 29.46, 26.5, 22.8, 14.3. HRMS (ASAP-TOF): Calculated for C$_{96}$H$_{123}$N$_2$O$_{12}^+$: 1495.9056. Found m/z 1495.9076 [M + H]$^+$.

Synthesis of N,N′-Bis(2-octyldodecyl)-2,5,8,11-tetrakis(2-resorcinol)perylene-3,4,9,10-tetracarboxylic Acid Diimide (PDI-OH). To a 25 mL μw vial under argon, BBr$_3$ (1 M in DCM, 5.34 mL) was added dropwise to a solution of PDI-OMe (400 mg, 0.2674 mmol) in anhydrous DCM (4.8 mL) at −78 °C. The reaction

was then left to warm to room temperature and stirred for 5 h. The reaction mixture was slowly poured into a prestirring saturated NaHCO$_3$ solution (∼200 mL), and it was extracted with DCM (2×). The organic phase was washed with brine, dried over MgSO$_4$, and concentrated and dried in vacuo to afford the product as a red solid (346.7 mg, 0.2505 mmol, 94% crude). The crude was used in the subsequent step without further purification. ^{1}H NMR (400 MHz, DMSO) δ 9.03 (s, 8H), 8.34 (s, 4H), 6.97 (t, J = 8.1 Hz, 4H), 6.41 (d, J = 8.2 Hz, 8H), 3.76 (d, J = 6.4 Hz, 4H), 1.76 (s, 2H), 1.19 (dd, J = 29.2, 7.7 Hz, 68H), 0.81 (dd, J = 7.0, 6.0 Hz, 12H). ^{13}C NMR{H} (125 MHz, DMSO) δ 162.1, 154.5, 141.2, 131.9, 130.3, 128.4, 127.9, 124.3, 121.7, 117.6, 106.7, 31.34, 31.30, 30.7, 30.6, 29.6, 29.40, 29.35, 29.1, 29.04, 29.02, 28.96, 28.7, 28.63, 25.57, 25.5, 22.09, 22.09, 14.0, 13.9. HRMS (MALDI-TOF): Calculated for C$_{88}$H$_{107}$N$_2$O$_{12}^+$: 1383.7819. Found m/z 1384.0034 [M + H]$^+$.

Synthesis of Double Encapsulated PDI (PDI-Encap). Under argon, PDI octa-ol (850 mg, 0.6142 mmol) and K$_2$CO$_3$ (1.6964 g, 12.2741 mmol) were stirred in dry DMF (170 mL) and heated to 50 °C for 1 h. Next, a solution of 1,8-dibromooctane (0.51 mL, 2.7692 mmol) in dry DMF (170 mL) was added dropwise, and the reaction mixture was heated to 80 °C for 48 h. The crude reaction mixture was concentrated in vacuo, absorbed onto silica and purified by silica column chromatography using DCM and hexane (30% DCM → 50% DCM in hexane). The product was obtained as an orange solid (43 mg, 0.0236 mmol, 4%). ^{1}H NMR (500 MHz, CDCl$_3$) δ 8.34 (s, 4H), 7.32 (t, J = 8.3 Hz, 4H), 6.74 (d, J = 8.3 Hz, 8H), 4.05−3.98 (m, 8H), 3.88 (d, J = 7.3 Hz, 4H), 3.76 (td, J = 9.1, 3.0 Hz, 8H), 1.80 (dt, J = 12.4, 6.1 Hz, 2H), 1.40 (ddd, J = 9.4, 8.5, 5.3 Hz, 12H), 1.23 (tdd, J = 19.0, 15.0, 6.7 Hz, 56H), 1.13−1.04 (m, 12H), 0.87 (td, J = 7.0, 4.0 Hz, 12H), 0.82−0.62 (m, 32H). ^{13}C NMR{H} (125 MHz, CDCl$_3$) δ 162.9, 156.6, 141.7, 133.2, 130.9, 129.0, 128.5, 125.5, 124.4, 121.6, 108.2, 70.7, 44.1, 36.2, 32.09, 32.08, 30.9, 30.7, 30.4, 30.2, 29.89, 29.85, 29.8, 29.54, 29.52, 27.8, 26.2, 22.8, 14.3. HRMS (ASAP-TOF): Calculated for C$_{120}$H$_{163}$N$_2$O$_{12}^+$: 1824.2201. Found m/z 1824.2170 [M + H]$^+$. Anal. Calcd. for C$_{120}$H$_{162}$N$_2$O$_{12}$: C, 78.99; H, 8.95; N, 1.54. Found: C, 78.83; H, 9.02; N, 1.72 (average of two runs).

■ ASSOCIATED CONTENT

ⓢ Supporting Information

The Supporting Information is available free of charge on the ACS Publications website at DOI: 10.1021/acs.joc.9b02597.

Crystallographic information files (CIF)

NMR spectra, photophysical data, computational data, and X-ray crystallography (PDF)

■ AUTHOR INFORMATION

Corresponding Author

*E-mail: hab60@cam.ac.uk.

ORCID ⓘ

Weixuan Zeng: 0000-0003-1577-9021

Andrew D. Bond: 0000-0002-1744-0489

Dejan-Krešimir Bučar: 0000-0001-6393-276X

Franco Cacialli: 0000-0001-6821-6578

Hugo Bronstein: 0000-0003-0293-8775

Notes

The authors declare no competing financial interest.

■ ACKNOWLEDGMENTS

■ REFERENCES

(1) Guo, X.; Facchetti, A.; Marks, T. J. Imide- and Amide-Functionalized Polymer Semiconductors. *Chem. Rev.* **2014**, *114* (18), 8943−9012.

(2) Huang, C.; Barlow, S.; Marder, S. R. Perylene-3, 4, 9, 10-Tetracarboxylic Acid Diimides: Synthesis, Physical Properties, and Use in Organic Electronics. *J. Org. Chem.* **2011**, *76* (8), 2386−2407.

(3) Wurthner, F.; Saha-Moller, C. R.; Fimmel, B.; Ogi, S.; Leowanawat, P.; Schmidt, D.; et al. Perylene Bisimide Dye Assemblies as Archetype Functional Supramolecular Materials. *Chem. Rev.* **2016**, *116* (3), 962−1052.

(4) Zhang, B.; Soleimaninejad, H.; Jones, D. J.; White, J. M.; Ghiggino, K. P.; Smith, T. A.; Wong, W. W. H. Highly Fluorescent Molecularly Insulated Perylene Diimides: Effect of Concentration on Photophysical Properties. *Chem. Mater.* **2017**, *29* (19), 8395−8403.

(5) Chen, Z.; Stepanenko, V.; Dehm, V.; Prins, P.; Siebbeles, L. D. A.; Seibt, J.; Marquetand, P.; Engel, V.; Würthner, F. Photoluminescence and Conductivity of Self-Assembled Π−π Stacks of Perylene Bisimide Dyes. *Chem. - Eur. J.* **2007**, *13* (2), 436−449.

(6) Idé, J.; Méreau, R.; Ducasse, L.; Castet, F.; Olivier, Y.; Martinelli, N.; Cornil, J.; Beljonne, D. Supramolecular Organization and Charge Transport Properties of Self-Assembled Π− π Stacks of Perylene Diimide Dyes. *J. Phys. Chem. B* **2011**, *115* (18), 5593−5603.

(7) Würthner, F. Perylene Bisimide Dyes as Versatile Building Blocks for Functional Supramolecular Architectures. *Chem. Commun.* **2004**, No. 14, 1564−1579.

(8) Schmidt, D.; Stolte, M.; Süß, J.; Liess, A.; Stepanenko, V.; Würthner, F. Protein-like Enwrapped Perylene Bisimide Chromophore as a Bright Microcrystalline Emitter Material. *Angew. Chem., Int. Ed.* **2019**, *58*, 13385−13389.

(9) Cai, Y.; Huo, L.; Sun, X.; Wei, D.; Tang, M.; Sun, Y. High Performance Organic Solar Cells Based on a Twisted Bay-Substituted Tetraphenyl Functionalized Perylenediimide Electron Acceptor. *Adv. Energy Mater.* **2015**, *5* (11), 1500032.

(10) Chen, Z.; Debije, M. G.; Debaerdemaeker, T.; Osswald, P.; Würthner, F. Tetrachloro-substituted Perylene Bisimide Dyes as Promising N-type Organic Semiconductors: Studies on Structural, Electrochemical and Charge Transport Properties. *ChemPhysChem* **2004**, *5* (1), 137−140.

(11) Osswald, P.; Leusser, D.; Stalke, D.; Würthner, F. Perylene Bisimide Based Macrocycles: Effective Probes for the Assessment of Conformational Effects on Optical Properties. *Angew. Chem., Int. Ed.* **2005**, *44* (2), 250−253.

(12) Banal, J. L.; Soleimaninejad, H.; Jradi, F. M.; Liu, M.; White, J. M.; Blakers, A. W.; Cooper, M. W.; Jones, D. J.; Ghiggino, K. P.; Marder, S. R. Energy Migration in Organic Solar Concentrators with a Molecularly Insulated Perylene Diimide. *J. Phys. Chem. C* **2016**, *120* (24), 12952−12958.

(13) Leventis, A.; Royakkers, J.; Rapidis, A. G.; Goodeal, N.; Corpinot, M. K.; Frost, J. M.; Bučar, D.-K. K.; Blunt, M. O.; Cacialli, F.; Bronstein, H. Highly Luminescent Encapsulated Narrow Bandgap Polymers Based on Diketopyrrolopyrrole. *J. Am. Chem. Soc.* **2018**, *140* (5), 1622−1626.

(14) Fujiwara, Y.; Ozawa, R.; Onuma, D.; Suzuki, K.; Yoza, K.; Kobayashi, K. Double Alkylene-Strapped Diphenylanthracene as a Photostable and Intense Solid-State Blue-Emitting Material. *J. Org. Chem.* **2013**, *78* (6), 2206−2212.

(15) Frampton, M. J.; Anderson, H. L. Insulated Molecular Wires. *Angew. Chem., Int. Ed.* **2007**, *46* (7), 1028−1064.

(16) Sugiyasu, K.; Honsho, Y.; Harrison, R. M.; Sato, A.; Yasuda, T.; Seki, S.; Takeuchi, M. A Self-Threading Polythiophene: Defect-Free Insulated Molecular Wires Endowed with Long Effective Conjugation Length. *J. Am. Chem. Soc.* **2010**, *132* (42), 14754−14756.

(17) Pan, C.; Sugiyasu, K.; Wakayama, Y.; Sato, A.; Takeuchi, M. Thermoplastic Fluorescent Conjugated Polymers: Benefits of Preventing π-π Stacking. *Angew. Chem., Int. Ed.* **2013**, *52* (41), 10775−10779.

(18) Sun, C.; Mróz, M. M.; Smirnov, J. R. C.; Lüer, L.; Hermida-Merino, D.; Zhao, C.; Takeuchi, M.; Sugiyasu, K.; Cabanillas-González, J. Amplified Spontaneous Emission in Insulated Polythiophenes. *J. Mater. Chem. C* **2018**, *6* (24), 6591−6596.

(19) Sugiyasu, K.; Takeuchi, M. Conducting Polymer Networks Cross-Linked by "Isolated" Functional Dyes: Design, Synthesis, and Electrochemical Polymerization of Doubly Strapped Light-Harvesting Porphyrin/Oligothiophene Monomers. *Chem. - Eur. J.* **2009**, *15* (26), 6350−6362.

(20) Shomura, R.; Sugiyasu, K.; Yasuda, T.; Sato, A.; Takeuchi, M. Electrochemical Generation and Spectroscopic Characterization of Charge Carriers within Isolated Planar Polythiophene. *Macromolecules* **2012**, *45* (9), 3759−3771.

(21) Pan, C.; Zhao, C.; Takeuchi, M.; Sugiyasu, K. Conjugated Oligomers and Polymers Sheathed with Designer Side Chains. *Chem. - Asian J.* **2015**, *10* (9), 1820−1835.

(22) Anderson, S.; Aplin, R. T.; Claridge, T. D. W.; Goodson, T., III; Maciel, A. C.; Rumbles, G.; Ryan, J. F.; Anderson, H. L. An Approach to Insulated Molecular Wires: Synthesis of Water-Soluble Conjugated Rotaxanes. *J. Chem. Soc., Perkin Trans. 1* **1998**, No. 15, 2383−2398.

(23) Battagliarin, G.; Li, C.; Enkelmann, V.; Müllen, K. 2, 5, 8, 11-Tetraboronic Ester Perylenediimides: A next Generation Building Block for Dye-Stuff Synthesis. *Org. Lett.* **2011**, *13* (12), 3012−3015.

(24) Teraoka, T.; Hiroto, S.; Shinokubo, H. Iridium-Catalyzed Direct Tetraborylation of Perylene Bisimides. *Org. Lett.* **2011**, *13* (10), 2532−2535.

(25) Walker, S. D.; Barder, T. E.; Martinelli, J. R.; Buchwald, S. L. A Rationally Designed Universal Catalyst for Suzuki−Miyaura Coupling Processes. *Angew. Chem., Int. Ed.* **2004**, *43* (14), 1871−1876.

(26) Gómez, R.; Veldman, D.; Blanco, R.; Seoane, C.; Segura, J. L.; Janssen, R. A. J. Energy and Electron Transfer in a Poly (Fluorene-Alt-Phenylene) Bearing Perylenediimides as Pendant Electron Acceptor Groups. *Macromolecules* **2007**, *40* (8), 2760−2772.

(27) Akimoto, S.; Ohmori, A.; Yamazaki, I. Dimer Formation and Excitation Relaxation of Perylene in Langmuir− Blodgett Films. *J. Phys. Chem. B* **1997**, *101* (19), 3753−3758.

(28) Barford, W.; Marcus, M. Perspective: Optical Spectroscopy in π-Conjugated Polymers and How It Can Be Used to Determine Multiscale Polymer Structures. *J. Chem. Phys.* **2017**, *146* (13), 130902.

(29) Panzer, F.; Bässler, H.; Köhler, A. Temperature Induced Order−disorder Transition in Solutions of Conjugated Polymers Probed by Optical Spectroscopy. *J. Phys. Chem. Lett.* **2017**, *8* (1), 114−125.

(30) Lakowicz, J. R. *Principles of Fluorescence Spectroscopy*; Springer Science & Business Media, 2013.

(31) Janiak, C. A. Critical Account on Π−π Stacking in Metal Complexes with Aromatic Nitrogen-Containing Ligands. *J. Chem. Soc. Dalt Trans* **2000**, No. 21, 3885−3896.

(32) Brown, K. E.; Salamant, W. A.; Shoer, L. E.; Young, R. M.; Wasielewski, M. R. Direct Observation of Ultrafast Excimer Formation in Covalent Perylenediimide Dimers Using near-Infrared Transient Absorption Spectroscopy. *J. Phys. Chem. Lett.* **2014**, *5* (15), 2588−2593.

(33) Schubert, A.; Settels, V.; Liu, W.; Würthner, F.; Meier, C.; Fink, R. F.; Schindlbeck, S.; Lochbrunner, S.; Engels, B.; Engel, V. Ultrafast Exciton Self-Trapping upon Geometry Deformation in Perylene-Based Molecular Aggregates. *J. Phys. Chem. Lett.* **2013**, *4* (5), 792−796.

(34) Sung, J.; Kim, P.; Fimmel, B.; Würthner, F.; Kim, D. Direct Observation of Ultrafast Coherent Exciton Dynamics in Helical π-Stacks of Self-Assembled Perylene Bisimides. *Nat. Commun.* **2015**, *6*, 8646.

(35) Sung, J.; Nowak-Król, A.; Schlosser, F.; Fimmel, B.; Kim, W.; Kim, D.; Würthner, F. Direct Observation of Excimer-Mediated Intramolecular Electron Transfer in a Cofacially-Stacked Perylene Bisimide Pair. *J. Am. Chem. Soc.* **2016**, *138* (29), 9029−9032.

(36) Becke, A. D. Density-Functional Exchange-Energy Approximation with Correct Asymptotic Behavior. *Phys. Rev. A: At., Mol., Opt. Phys.* **1988**, *38* (6), 3098.

(37) Chen, Z.; Zheng, Y.; Yan, H.; Facchetti, A. Naphthalenedicarboximide- vs Perylenedicarboximide-Based Copolymers. Synthesis and Semiconducting Properties in Bottom-Gate N-Channel Organic Transistors. *J. Am. Chem. Soc.* **2009**, *131* (1), 8–9.